SLAC-PUB-2387
LBL-9502
August 1979
(M)

RESULTS FROM THE MARK II DETECTOR AT SPEAR

G. S. Abrams, M. S. Alam, C. A. Blocker, A. M. Boyarski, M. Breidenbach, C. H. Broll, D. L. Burke, W. C. Carithers, W. Chinowsky, M. W. Coles, S. C. Cooper, W. E. Dieterle, J. W. Dillon, J. Dorenbosch, J. M. Dorfan, M. W. Eaton, G. J. Feldman, H. G. Fischer, M. E. B. Franklin, G. Gidal, G. Goldhaber, G. Hanson, K. G. Hayes, T. Himel, D. G. Hitlin, R. J. Hollebeek, W. R. Innes, J. A. Jaros, P. Jenni, A. D. Johnson, J. A. Kadyk, A. J. Lankford, R. R. Larsen, D. Lüke, V. Lüth, J. F. Martin, R. E. Millikan, M. Nelson, C. Y. Pang, J. F. Patrick, M. L. Perl, B. Richter, J. J. Russell, D. L. Scharre, R. H. Schindler, R. F. Schwitters, S. R. Shannon, J. L. Siegrist, J. Strait, H. Taureg, M. Tonutti, G. H. Trilling, E. N. Vella, R. A. Vidal, M. I. Videau, J. M. Weiss, and H. Zaccone

(presented by G. Gidal†)

Stanford Linear Accelerator Center, Stanford, CA 94305
and
†Lawrence Berkeley Laboratory, Berkeley, CA 94720

ABSTRACT

We present some recent results from the Mark II detector at SPEAR:* (1) observation of some new D meson decay modes, including the Cabibbo suppressed K^-K^+ and $\pi^-\pi^+$ modes, (2) measurements of the $\rho\nu$ and $\pi\nu$ decays of the τ, and (3) some new data on ψ decays.

The Mark II detector has been in operation at SPEAR since the end of 1977 and has accumulated data over a wide range of energies between the $\psi(3100)$ and 7.4 GeV. Figure 1 shows the integrated luminosity as a function of E_{cm}. The logarithmic scale is used to indicate large runs at several energies in addition to systematic scans.

A schematic drawing of the detector is shown in Figure 2. Moving outward from the interaction region, the detector consists of two layers of cylindrical scintillation counters, 16 layers of cylindrical drift chambers,[1] 48 scintillation counters for time of flight (TOF), an aluminum solenoidal coil which produces a 4.1 kg axial magnetic field, 8 lead-liquid argon barrel shower counters,[2] iron hadron absorbers and two planes of proportional tubes, covering 55% of the solid angle, for muon detection. There are also shower detectors in the endcap regions: one of lead and liquid argon, and the other of two layers of lead and proportional chambers. The most common trigger[3] requires at least one charged track to be within the central 75% of the solid angle and a second charged track within approximately 85% of the solid angle.

The performance of the major components of the detector can be summarized as follows. The drift chambers measure the azimuthal coordinates of charged tracks to a rms accuracy of 200 μ at each layer. When tracks are constrained to pass through the known beam position, the rms momentum resolution can be parametrized as $\delta p/p = [(0.005\,p)^2 + (0.0145)^2]^{1/2}$, where p is measured in GeV/c. The tracking efficiency is greater than 95% for tracks with

*Work supported in part by the High Energy Physics Division of the U.S. Department of Energy under contract number W-7405-ENG-48 and in part by the Department of Energy under contract number DE-AC03-76SF00515.

(Invited talk presented at the 1979 EPS High Energy Physics Conference, Geneva, Switzerland, June 27 - July 4, 1979.)

$p > 100$ MeV/c over 75% of 4π sr. Figure 3 shows the difference between the expected time and the measured time for 2.08 GeV Bhabhas and is fit by a Gaussian with $\sigma = .270$ ns. For hadrons, the rms resolution is closer to .300 ns and leads to a 1σ separation between π's and K's at 1.35 GeV/c and between K's and p's at 2.0 GeV/c. Figure 4a shows the energy dependence of the γ detection efficiency of the Liquid Argon barrel shower counters. This is measured with the reactions $\psi \to \pi^+\pi^-\pi^o$ and $\psi \to 2\pi^+2\pi^-\pi^o$ in which one observed γ is used to predict the position of the other γ. This γ efficiency, together with the geometric acceptance, then translates into the π^o and η^o detection efficiencies shown in Figure 4b. The energy resolution of the Liquid Argon barrel modules is given by $\delta E/E = \frac{0.115}{\sqrt{E}}$ as measured by Bhabhas. The electron identification efficiency varies from .64 around 450 MeV/c, to .82 around 800 MeV/c, to .97 above 1.6 GeV.

I. New D meson decay modes

We report the first observation of Cabibbo suppressed decays of charmed particles. In the standard model, with SU(3) in variance, one predicts

$$\frac{\Gamma(D^o \to K^-K^+)}{\Gamma(D^o \to K^-\pi^+)} = \frac{\Gamma(D^o \to \pi^-\pi^+)}{\Gamma(D^o \to K^-\pi^+)} = \tan^2\theta_c \approx .05 \ .$$

To study the D decays we primarily depend on the 2840 nb^{-1} accumulated at 3.771 GeV (ψ''). Since D's are produced in pairs at this energy, oppositely charged track pairs with net momentum in the range 288 ± 30 MeV/c were selected as candidates for two body decays.

The TOF system provides about a 2.5σ separation between π's and K's at the 850 MeV/c particle momentum typical of such decays. The probability that each track is a π or a K is assigned from the TOF, and, the product of the individual probabilities for a given final state hypothesis was required to be greater than 0.3. The corresponding two body invariant mass spectra are shown in Figure 5. Correctly identified D^o's appear near 1863 MeV/c^2, while D^o's in which one particle has been misidentified will appear shifted by ~120 MeV/c^2. In addition to the dominant $K^\pm\pi^\mp$ decay mode, a clear K^-K^+ signal is seen and there is an excess of $\pi^-\pi^+$ events in the D^o region. Figure 6 shows the same events as a scatter plot of the measured invariant mass against the beam constrained mass[4]. A likelihood fit to the signals and estimated backgrounds give 234.5 ± 15.8 $K^\pm\pi^\mp$ decays, 22.1 ± 5.2 K^+K^- decays, and 9.3 ± 3.9 $\pi^+\pi^-$ decays. Introducing the relative efficiencies gives

$$\frac{\Gamma(D^o \to K^-K^+)}{\Gamma(D^o \to K^-\pi^+)} = .113 \pm .030 \quad \text{and} \quad \frac{\Gamma(D^o \to \pi^-\pi^+)}{\Gamma(D^o \to K^-\pi^+)} = .033 \pm .015$$

We have also looked at the two body decays from the data taken in the region of $\sqrt{s}$ between 3.8 and 4.5 GeV. Here we also required a recoil mass > 1.8 GeV and p_K < 1.3 GeV/c. For events satisfying each mass hypothesis, the two body invariant mass and the recoil mass spectrum for events lying in the three central D^o mass bins are shown in Figure 7. In the $K^{\pm}\pi^{\mp}$ channel, the familiar DD, DD^*, and D^*D^* peaks are evident in the recoil spectrum. The K^+K^- channel recoil spectrum shows the same structure. The shaded regions correspond to the 45 K^+K^- events above background predicted from our measurement of $\Gamma(D^o \to K^+K^-)$ above. This higher energy data thus qualitatively confirms the observation of the K^+K^- Cabbibo suppressed decay. The $\pi^+\pi^-$ recoil distribution does not obviously show the characteristic structure and so it would be difficult to attribute all 39 shaded $\pi^+\pi^-$ events above the estimated background to $D^o \to \pi^+\pi^-$. The background uncertainties prohibit the use of this data to obtain precise branching fractions.

To study other decay modes of the D meson we again rely on the relatively background-free invariant mass spectra obtained with the ψ'' data. Figure 8 shows the beam constrained mass plots for the D decay channels $K^{\pm}\pi^{\mp}\pi^o$, $K^o\pi^-\pi^+$, $K^o\pi^o$, $K^o\pi^{\pm}$, and $K^o\pi^{\pm}\pi^{\pm}\pi^{\mp}$. The K^o's are detected from their $\pi^+\pi^-$ decay with an efficiency of $\approx$ 35% and are constrained to the K^o mass. The π^o's are reconstructed from 2 observed γ's whose energies are adjusted to give the π^o mass. An additional cut on the difference between the observed mass and the recoil mass is made before beam constraint. All these modes are seen, with resolutions well described by the Monte Carlo program.

The sensitivity of this experiment to the decay mode $D^o \to \bar{K}^o\pi^o$ is ~1/25 that for $D^o \to K^-\pi^+$, giving a (preliminary) value for the ratio

$$\frac{\Gamma(D^o \to K^-\pi^+)}{\Gamma(D^o \to \bar{K}^o\pi^o)} = 1.6 \pm 0.9$$

Most theoretical estimates[5] of charmed meson hadronic decay rates include the assumption of color selection, highly suppressing D^o decays into $\bar{K}^o$ or $\bar{K}^{*o}$ with respect to D^o decays into K^- or K^{*-}. On the other hand, Fritzsch[15] has recently argued that such color selection rules can easily be invalidated by the emission or absorption of soft gluons, predicting ~2 for the above ratio.

II. The ρν and πν decays of the τ

Oppositely charged two prongs with coplanarity angle >20° were selected from the data in the $\sqrt{s}$ region between 4.5 and 6.0 GeV. For the ρν decay we also require two photons detected in the barrel modules. Figure 9 shows the γγ invariant mass for accepted photons and indicates a large π^o signal. We require $M(\gamma\gamma) < 200$ MeV/c^2 and adjust the γ energies to the π^o mass constraint ($\chi^2 < 6.0$/1df). The TOF, Liquid Argon, and muon systems were used when possible to identify the charged particles as kaon, proton, muon, or electron. All other tracks were called $\pi^{\pm}$. Figure 10a then shows the $\pi^{\pm}\pi^o$ invariant mass. Figure 10b shows the same distribution for events in which one of the charged tracks is a lepton. A clear ρ signal is observed. Because the lepton requirement insures only one entry per event and adds credence to the supposition that the ρ's come from τ decays, we concentrate on the ρ-lepton events to obtain a branching fraction. Events are normalized to eμ events in the same data sample. The solid curve in Figure 10b is the result of a fit to the data in the flat background + a Breit Wigner. The Monte Carlo used to obtain the efficiency assumes that the ρ's have two origins: $\tau \to \rho\nu$ and $\tau \to (A_1\nu + 4\pi$ continuum). The efficiency for detecting ρe events is 6.4%, for detecting ρμ events is 2.7%, and for detecting eμ events is 12.9%. Taking all events in Figure 10b as ρ-lepton, there are 64 ρe events and 21 ρμ events. After background subtraction (~10%) this gives

$$BR_{\tau\to\rho\nu} \cdot BR_{\tau\to e\nu\bar{\nu}} = .0435 \pm .0085$$

$$BR_{\tau\to\rho\nu} \cdot BR_{\tau\to\mu\nu\bar{\nu}} = .0329 \pm .0100$$

$$\sqrt{BR_{\tau\to e\nu\bar{\nu}} \cdot BR_{\tau\to\mu\nu\bar{\nu}}} = 18.5 \pm 1.2\% \quad ;$$

with μ-e universality this gives

$$BR_{\tau\to\rho\nu} = (21.1 \pm 3.7)\%$$

and

$$\frac{BR_{\tau\to\rho\nu}}{BR_{\tau\to e\nu\bar{\nu}}} = 1.14 \pm 0.22$$

in excellent agreement with the theoretical prediction of Gilman and Miller[16] of 1.20, providing a check of the vector part of the weak coupling. The momentum spectrum of the 85 ρ lepton events is compared with the Monte Carlo prediction in Figure 11 and shows excellent agreement.

To study the $\pi\nu$ decay we also require the "pion" track to be positively identified by the muon system, and that there be no detected γ's with E > 100 MeV. This leaves 443 such πx events. The principal source of background is feed-down from the reactions $\tau^{\pm} \to \rho^{\pm}\nu$, $A_1^{\pm}\nu$, continuum. The Monte Carlo program is used to subtract this ~40% background in each pion momentum bin. The pion energy spectrum for the remaining events is shown in Figure 12. A Monte Carlo simulation of $\tau \to \pi\nu$ gives the distribution shown as the solid line, and a branching ratio

$$BR_{\tau\to\pi\nu} = (10.6 \pm 1.9)\% \quad ,$$

The comparison with previously reported results is shown in Table I.

III. Some decays of the ψ

We have accumulated ~430 nb^{-1} at the ψ -- half with the LA shower counters, half without. For the data with shower counter information, events with two charged prongs and at least 2 observed γ's were fit with SQUAW to the hypothesis $\psi \to \pi^+\pi^-\gamma\gamma$. TOF information was used to eliminate tracks other than pions. The $\gamma\gamma$ invariant mass is shown in Figure 13a and exhibits a clean π^o peak with a σ of 10 MeV. The $\pi^+\pi^-$ invariant mass distribution is shown in Figure 13b. The recoiling γ's are required to form a π^o ($.12 < M_{\gamma\gamma} < .15$ GeV), and events with charged ρ's ($0.60 < M_{\pi^+\pi^o} < 0.90$ GeV) are eliminated. A ρ^o peak is clearly seen. In Figure 13c we show the $\pi^+\pi^-\gamma$ invariant mass with π^o's eliminated. A clean η' signal is observed. The resulting branching ratios are given in Table II and compared to other measurements.

This work is supported by the U.S. Department of Energy under contract number W-7405-ENG-48 .

Table I

Summary of τ Decay Measurements

	This Experiment	Previous Measurements	
$BR_{\tau\to\rho\nu}$	(21.1 ± 3.7)%	(24 ± 9)%	(ref. 9)
$BR_{\tau\to\pi\nu}$	(10.6 ± 1.9)%	(9 ± 3.8)%	(ref. 6)
		(8 ± 3.5)%	(ref. 7)
		(9.3 ± 3.9)%	(ref. 8)

Table II

Measured Branching Fractions for $\psi \to \rho\pi$ and $\psi \to \eta'\gamma$

Decay Mode	This Measurement	Previous Measurements	
$BR(\psi\to\eta'\gamma)$	$3.4 \pm 0.7 \times 10^{-3}$	$3.8 \pm 1.3 \times 10^{-3}$	(ref. 10)
		$2.2 \pm 1.7 \times 10^{-3}$	(ref. 11)
		$2.4 \pm 0.7 \times 10^{-3}$	(ref. 12)
$BR(\psi\to\rho\pi)$	0.0132 ± 0.0021	0.010 ± 0.002	(ref. 12)
		0.012 ± 0.003	(ref. 13)
		0.013 ± 0.003	(ref. 14)
$\Gamma(\rho^0\pi^0)/\Gamma(\rho^\pm\pi^\mp)$	0.56 ± 0.06	0.63 ± 0.22	(ref. 12)
		0.59 ± 0.17	(ref. 14)

References

*Results on the radiative decays of the $\psi'(3684)$ and on inclusive baryon production were presented by J. M. Weiss elsewhere in these proceedings.

1. W. Davies-White et al., SLAC preprint SLAC-PUB-2181 (1978), to be published in Nucl. Instr. Meth.
2. G. S. Abrams et al., IEEE Trans. on Nucl. Sci. NS-25, 309 (1978).
3. M. Breidenbach, et al., IEEE Trans. NS-25, 706 (1978).

   H. Brafman, et al., IEEE Trans. NS-25, 692 (1978).
4. By "beam constrained mass" we mean $(E_B^2 - p^2)^{\frac{1}{2}}$, where p is the measured total momentum of the decay particles and E_B is the known beam energy.
5. N. Cabibbo and L. Maiani, Phys. Lett. 73B, 418 (1978).

   D. Fakirov and B. Stech, Nucl. Phys. B133, 315 (1978).
6. G. Alexander et al., Phys. Lett. 78B, 162 (1978).
7. W. Bacino et al., Phys. Rev. Lett. 42, 6 (1979).
8. G. Feldman et al., Int. Conf. on Neutrino Physics -- Neutrinos 78, p. 647, E. C. Fowler, ed. (Purdue University).
9. S. Yamada, Proc. of 1977 Int. Symp. on Lepton and Photon Interactions, Hamburg, 1977, p. 69.
10. D. L. Scharre, SLAC preprint SLAC-PUB-2321 (1979).
11. W. Braunschweig et al., Phys. Lett. 67B, 243 (1977).
12. W. Bartel et al., Phys. Lett. 64B, 483 (1976).
13. W. Braunschweig et al., Phys. Lett. 63B, 487 (1976).
14. B. Jean-Marie et al., Phys. Rev. Lett. 36, 291 (1976).
15. H. Fritzsh, CERN Ref. Th. 2648, 28 March 1979 (unpublished)
16. F.J.Gilman and D.H.Miller, Phys.Rev. D17, 1846(1978) and private communication.

Figure Captions

Figure 1. Integrated luminosity for Mark II detector at SPEAR, 1977-1979.

Figure 2. Schematic drawing of the Mark II detector looking along the incident beams. The side muon detectors and the endcap shower counters are not shown.

Figure 3. Difference between expected and measured time at TOF system for Bhabha events at $E_{cm} = 4.16$ GeV. The curve represents the expected distribution for 0.270 ns resolution.

Figure 4a. Measured energy dependence of γ detection efficiency. Curve is a Monte Carlo calculation.

4b. The π^o and η^o detection efficiences. Geometry (seven LA barrel modules in this case) and branching fractions are included. Data points are measured π^o values; curves are Monte Carlo calculations.

Figure 5. Invariant mass of two particle combinations which have a momentum within 30 MeV/c of the expected D^o momentum and TOF information consistent with the indicated particle masses.

Figure 6. Invariant mass (M_I) vs. beam constrained mass (M_c) for the K^+K^- and $\pi^+\pi^-$ mass assignments. The rectangular area was chosen from equivalent $K^\pm\pi^\mp$ mass plot.

Figure 7. Two body invariant mass and recoil mass spectrum against D ($1.84 < M < 1.90$), for each two body mass hypothesis. Data has $\sqrt{s}$ between 3.8 and 4.5 GeV.

Figure 8. Beam constrained mass spectra for some D meson decay channels: (a) $K^o\pi^\pm$, (b) $K^o\pi^+\pi^-$, (c) $K^o\pi^o$, (d) $K^o\pi^\pm\pi^\pm\pi^\mp$, and (e) $K^\pm\pi^\mp\pi^o$.

Figure 9. γ-γ mass for acoplanar 2 prongs.

Figure 10. $M(\pi^\pm\pi^o)$ for (a) all acoplanar two prong events with π^o and (b) those events in which the other charged track is identified as a lepton.

Figure 11. Momentum spectrum for rho candidates.

Figure 12. Pion energy spectrum for acoplanar πx events.

Figure 13. Invariant mass distributions for events which fit $\psi \to \pi^+\pi^-\gamma\gamma$. (a) $\gamma\gamma$ mass, (b) $\pi^+\pi^-$ mass recoiling against π^o with $\rho^\pm$ candidates removed, (c) $\pi^+\pi^-\gamma$ mass with events containing a π^o removed.

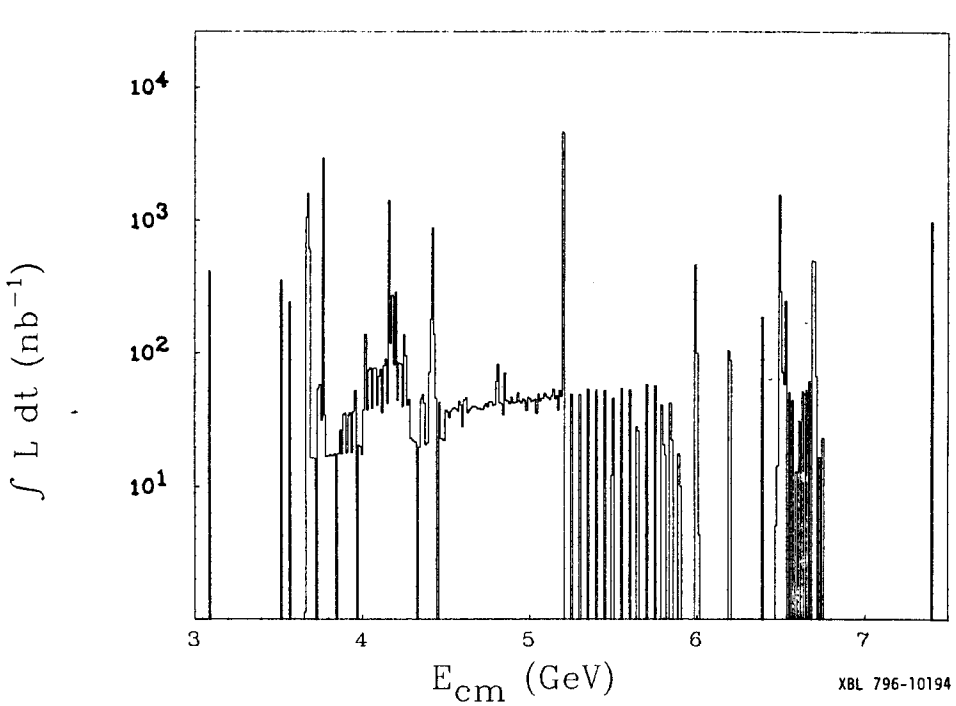

Figure 1

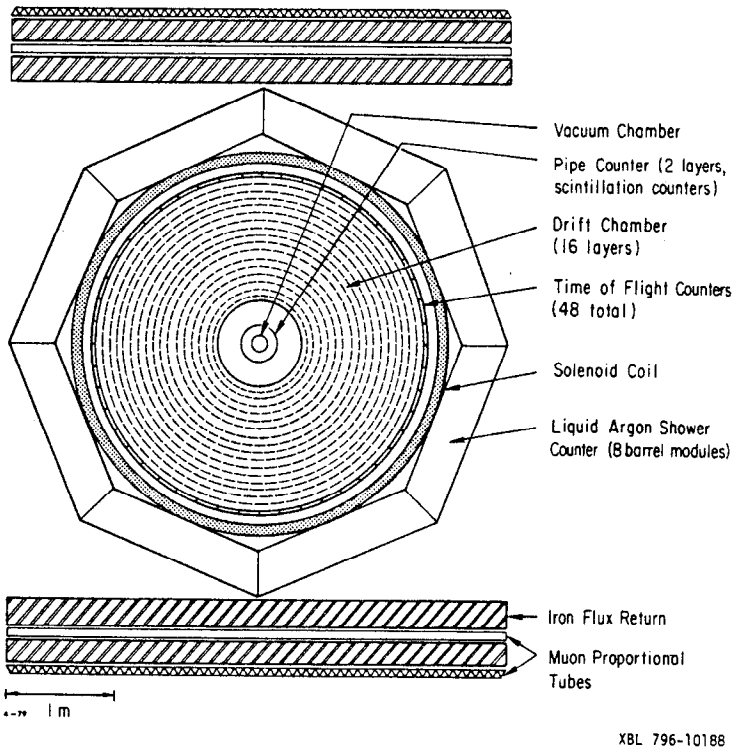

Figure 2

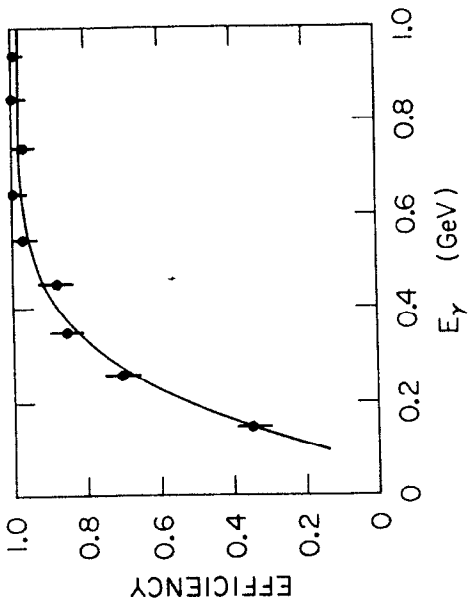

Figure 4a

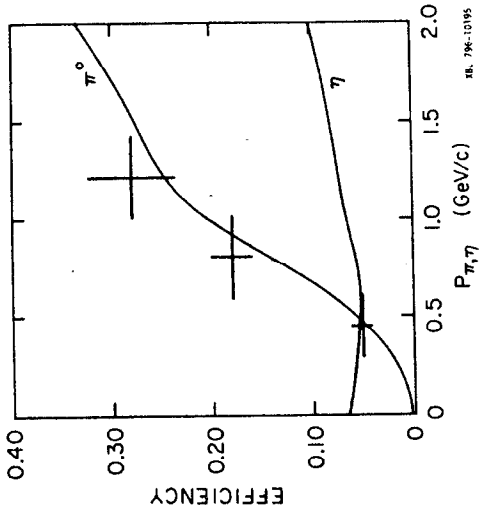

Figure 4b

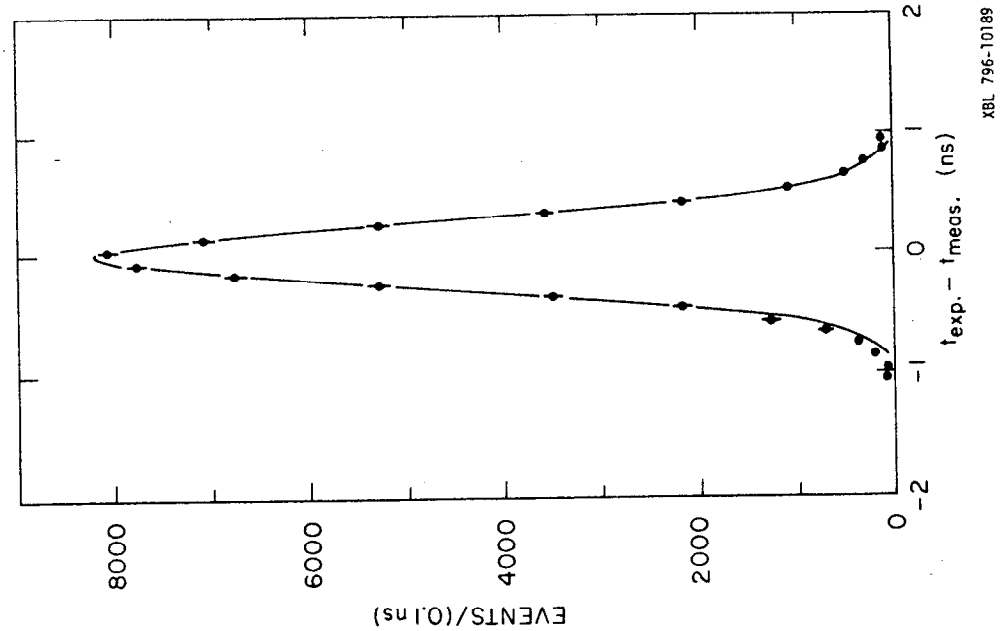

Figure 3

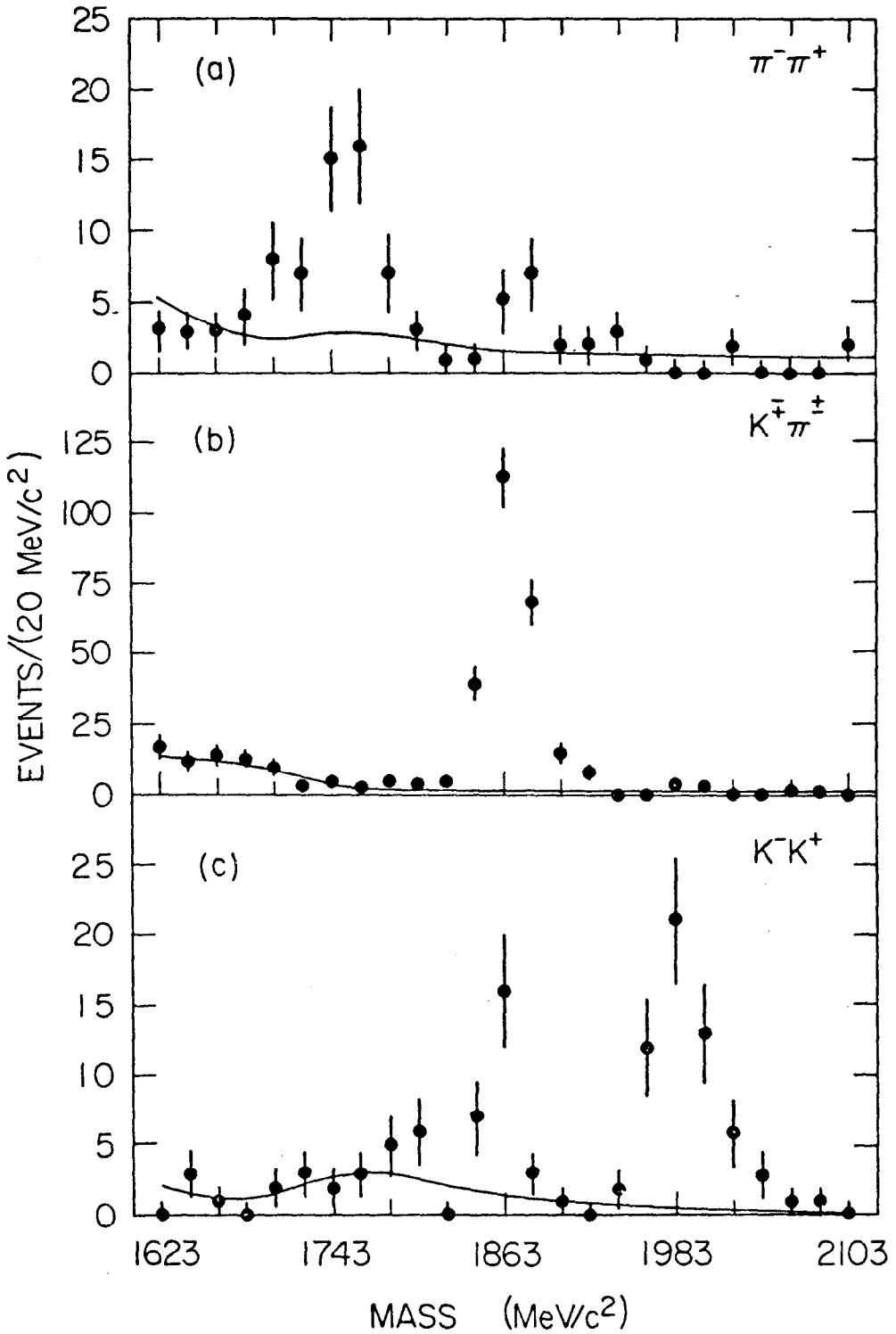

XBL 796-10190

Figure 5

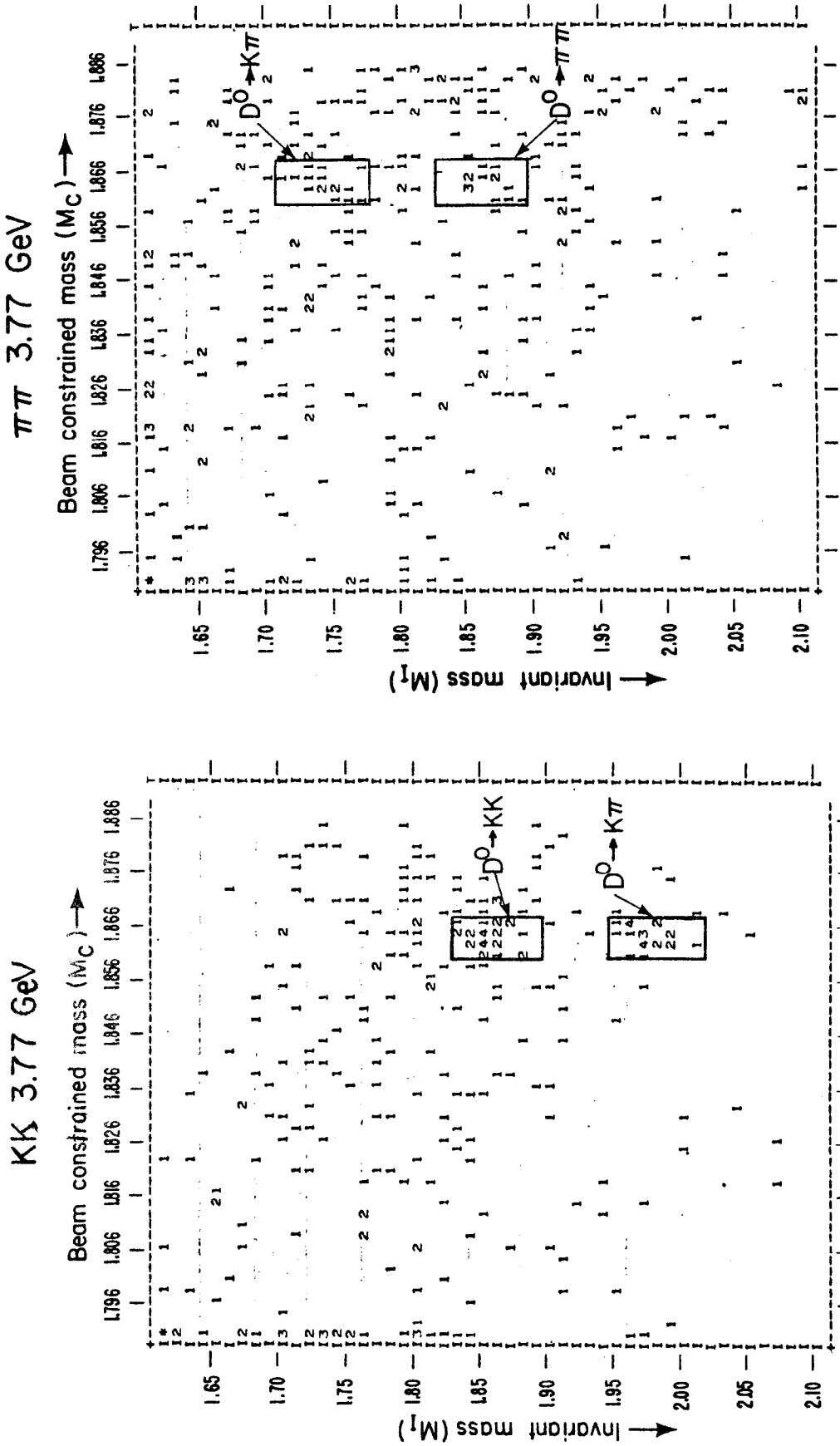

Figure 6b

XBL 796-805

Figure 6a

XBL 796-810

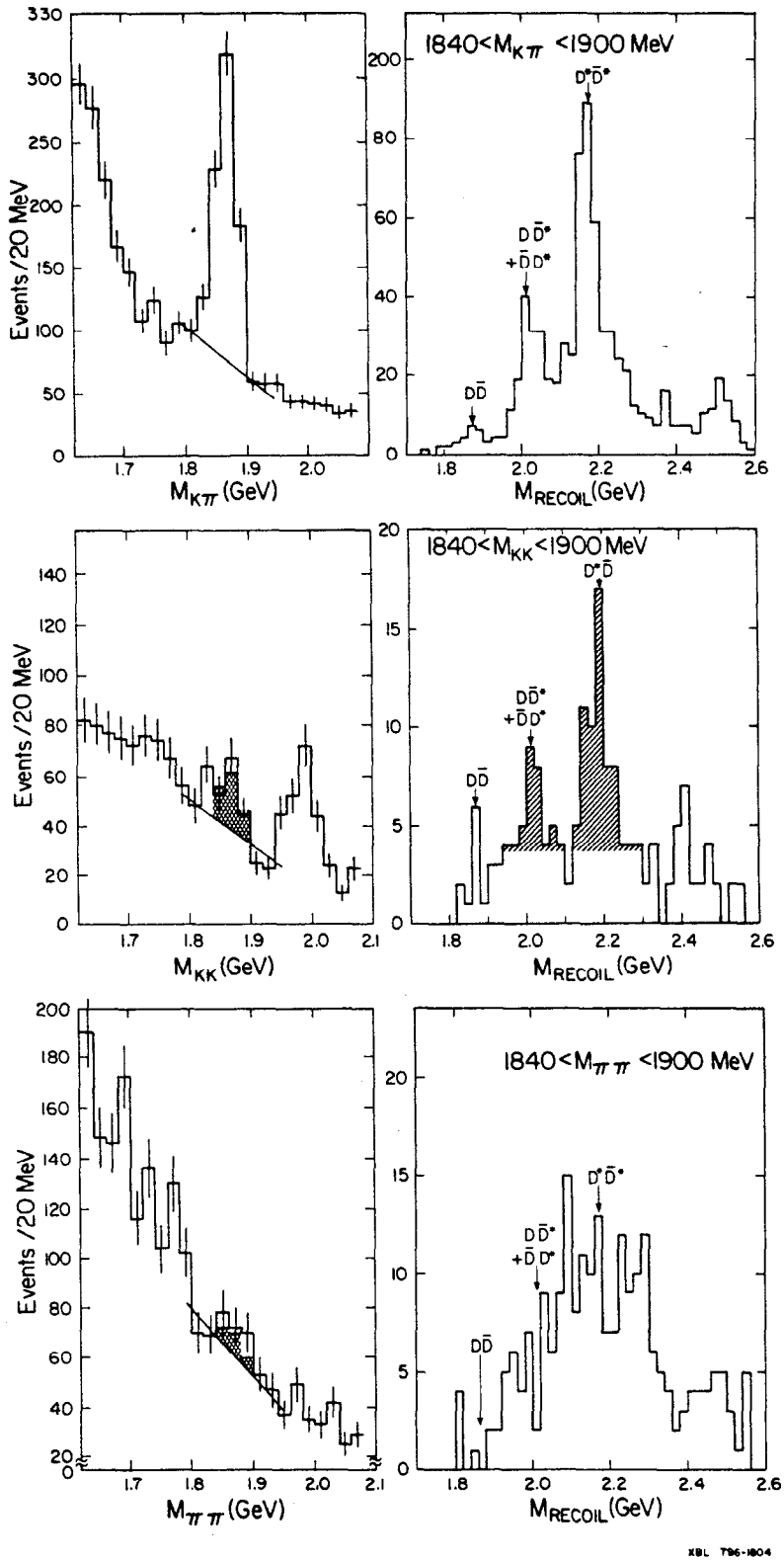
1840<M$_{K\pi}$ <1900 MeV
Events/20 MeV
M$_{K\pi}$ (GeV)
M$_{RECOIL}$(GeV)
D$\bar{D}$
D$\bar{D}^*$ +$\bar{D}$D*
D$^*\bar{D}^*$
1840<M$_{KK}$<1900 MeV
M$_{KK}$(GeV)
D$^*\bar{D}$
1840<M$_{\pi\pi}$ <1900 MeV
M$_{\pi\pi}$(GeV)
XBL 796-1804

Figure 7

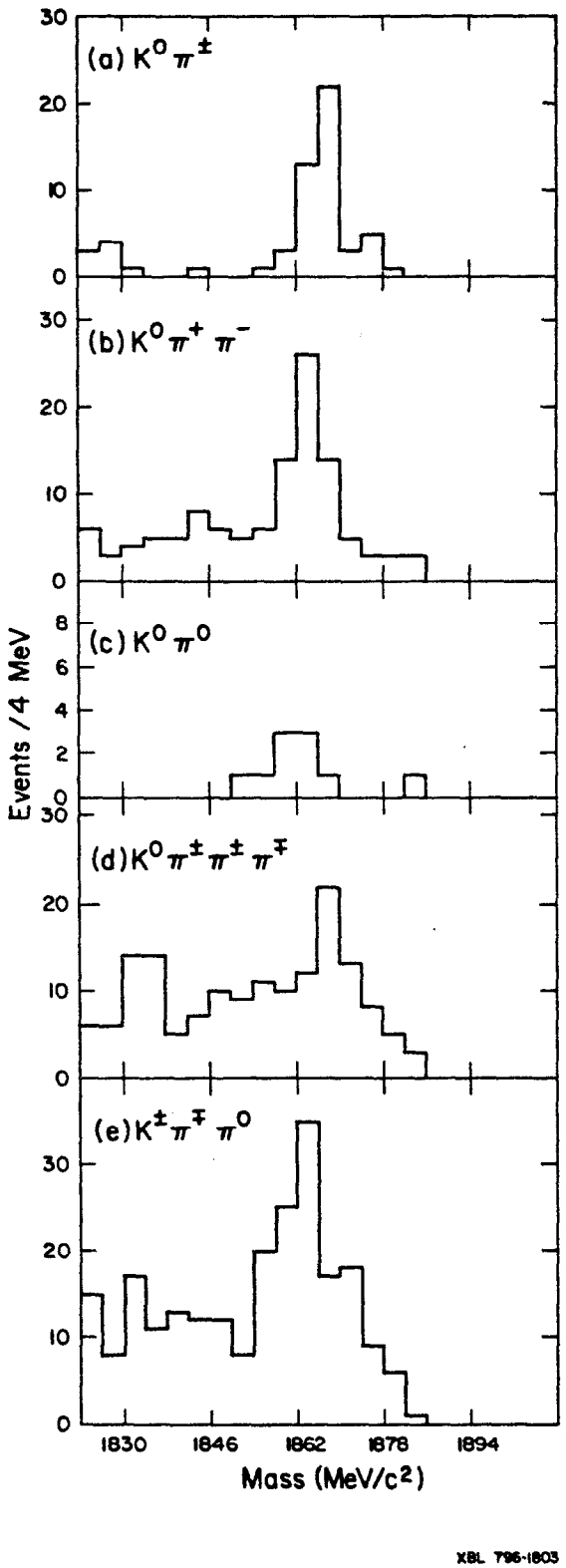
(a) $K^0\pi^\pm$
(b) $K^0\pi^+\pi^-$
(c) $K^0\pi^0$
(d) $K^0\pi^\pm\pi^\pm\pi^\mp$
(e) $K^\pm\pi^\mp\pi^0$
Events /4 MeV
Mass (MeV/c²)
1830
1846
1862
1878
1894
XBL 796-1803

Figure 8

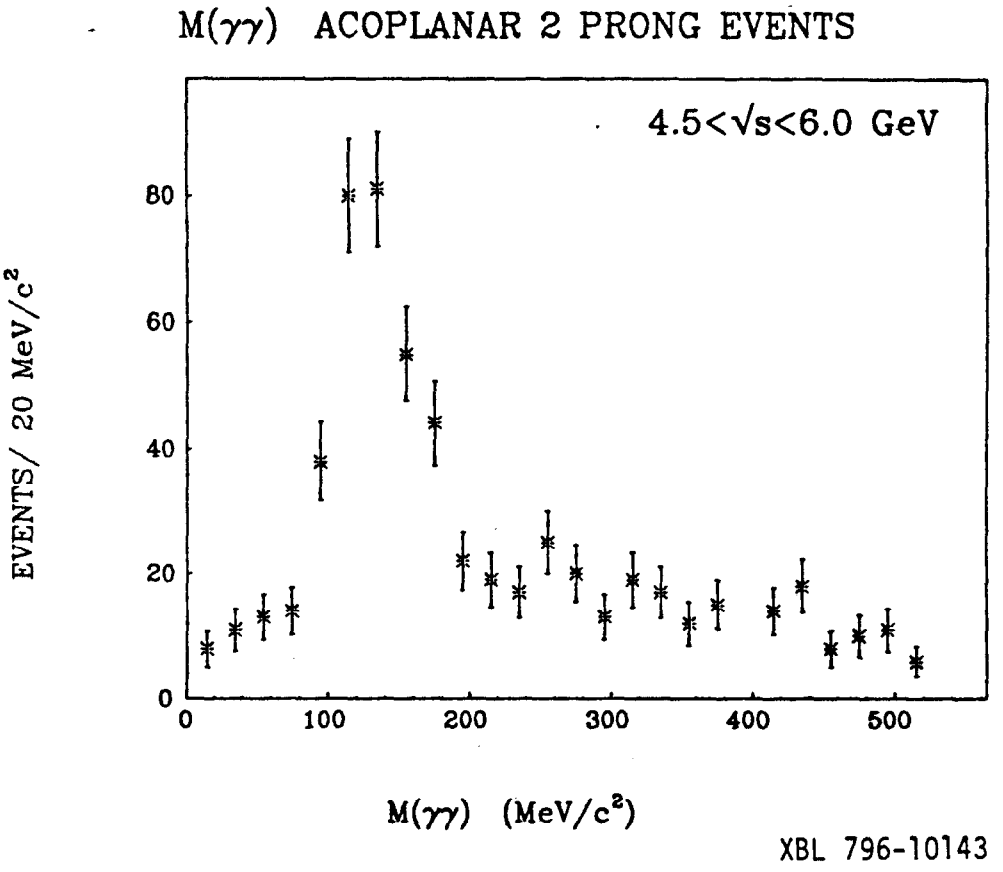
M(γγ) ACOPLANAR 2 PRONG EVENTS
4.5<√s<6.0 GeV
EVENTS/ 20 MeV/c²
0
20
40
60
80
0
100
200
300
400
500
M(γγ) (MeV/c²)
XBL 796-10143

Figure 9

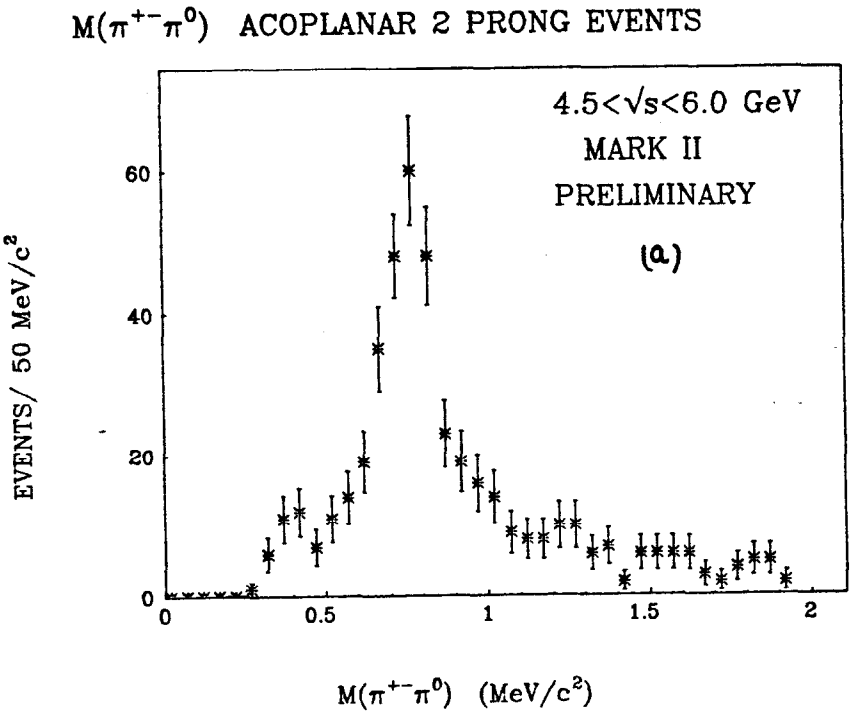

Figure 10a

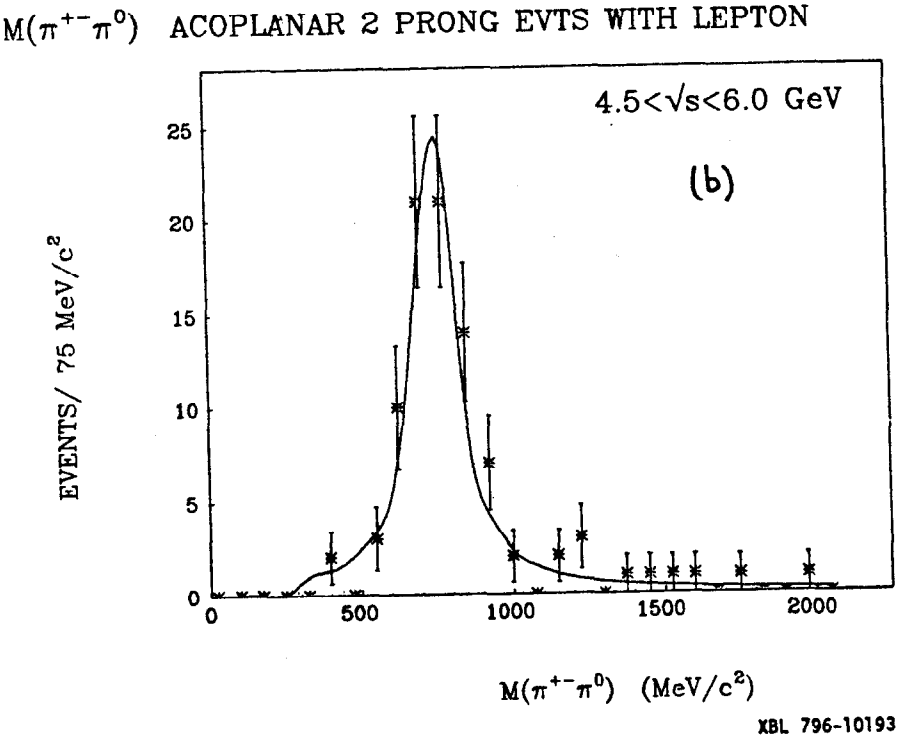

Figure 10b

MOMENTUM SPECTRUM FOR RHO CANDIDATES.

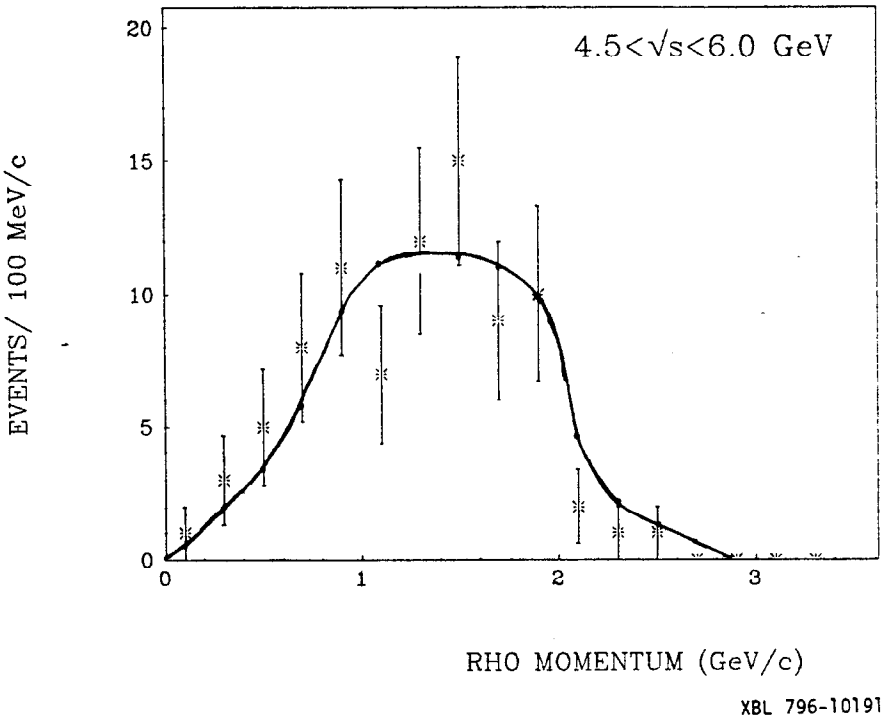

XBL 796-10191

Figure 11

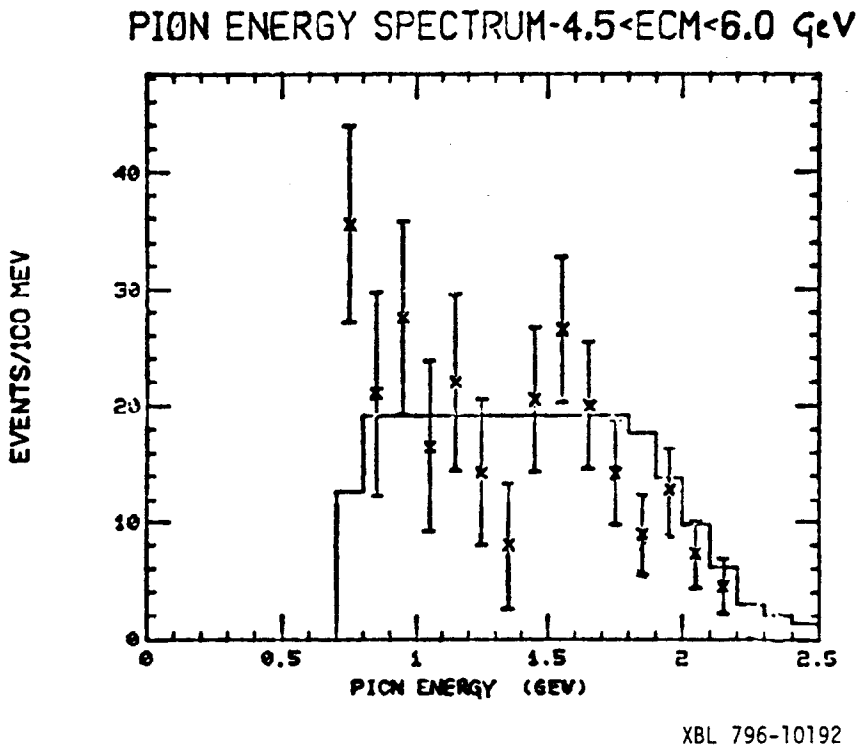

XBL 796-10192

Figure 12

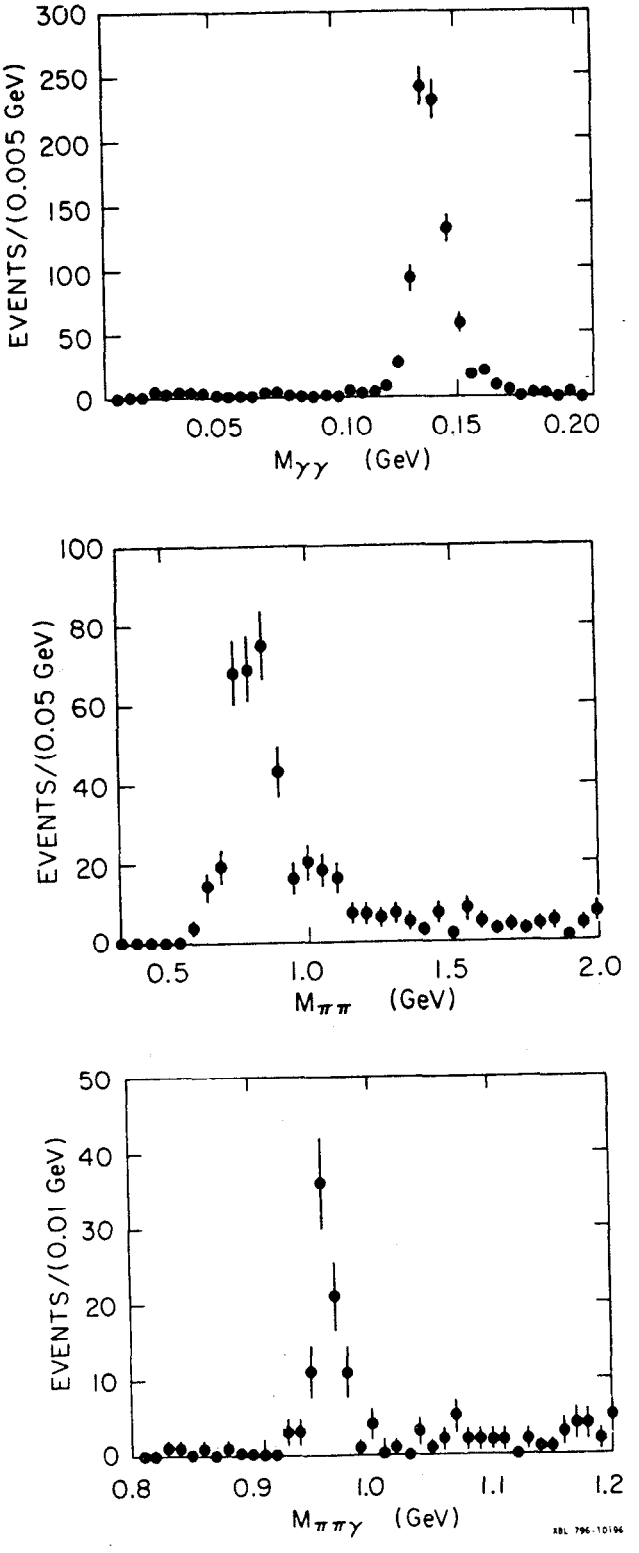
EVENTS/(0.005 GeV)
300
250
200
150
100
50
0
0.05
0.10
0.15
0.20
$M_{\gamma\gamma}$ (GeV)
EVENTS/(0.05 GeV)
100
80
60
40
20
0
0.5
1.0
1.5
2.0
$M_{\pi\pi}$ (GeV)
EVENTS/(0.01 GeV)
50
40
30
20
10
0
0.8
0.9
1.0
1.1
1.2
$M_{\pi\pi\gamma}$ (GeV)

Figure 13